

First-principles study of the band gap tuning and doping control in $CdSe_xTe_{1-x}$ alloy for high efficiency solar cell

Jingxiu Yang(杨竞秀), Su-Huai Wei(魏苏淮)

Citation: Chin. Phys. B . 2019, 28(8): 086106 . **doi:** 10.1088/1674-1056/28/8/086106
Journal homepage: http://cpb.iphy.ac.cn; http://iopscience.iop.org/cpb

What follows is a list of articles you may be interested in

Theoretical derivation of the crystallographic parameters of polytypes of long-period stacking ordered structures with the period of 13 and 14 in hexagonal close-packed system

Li Ye(叶礼), Dong-Shan Zhao(赵东山), Yuan-Lin Zhuang(庄园林), Shuang-Feng Jia(贾双凤), Jia-Ping Zhou(周嘉萍), Jia-Nian Gui(桂嘉年), Jian-Bo Wang(王建波)
Chin. Phys. B . 2018, 27(9): 096102 . **doi:** 10.1088/1674-1056/27/9/096102

Bandgap engineering to tune the optical properties of $Be_xMg_{1-x}X$ (X=S, Se, Te) alloys

B Sabir, N A Noor, M Rashid, Fasih Ud Din, Shahid M Ramay, Asif Mahmood
Chin. Phys. B . 2018, 27(1): 016101 . **doi:** 10.1088/1674-1056/27/1/016101

Molecular dynamics simulations of cascade damage near the $Y_2Ti_2O_7$ nanocluster/ferrite interface in nanostructured ferritic alloys

Yi-Qiang Sun(孙祎强), Wen-Sheng Lai(赖文生)
Chin. Phys. B . 2017, 26(7): 076106 . **doi:** 10.1088/1674-1056/26/7/076106

Effect of thermo-mechanical process on structure and high temperature shape memory properties of Ti-15Ta-15Zr alloy

Xiao-Hang Zheng(郑晓航), Jie-He Sui(隋解和), Zhe-Yi Yang(杨哲一), Guo-Zhang Zhi(张治国), Wei Cai(蔡伟)
Chin. Phys. B . 2017, 26(5): 056103 . **doi:** 10.1088/1674-1056/26/5/056103

Theoretical prediction of new C-Si alloys in *C*2/*m*-20 structure

Xiangyang Xu(徐向阳), Changchun Chai(柴常春), Qingyang Fan(樊庆扬), Yintang Yang(杨银堂)
Chin. Phys. B . 2017, 26(4): 046101 . **doi:** 10.1088/1674-1056/26/4/046101

RAPID COMMUNICATION

First-principles study of the band gap tuning and doping control in $CdSe_xTe_{1-x}$ alloy for high efficiency solar cell*

Jingxiu Yang(杨竞秀)[1,2] and Su-Huai Wei(魏苏淮)[2,†]

[1] *Department of Materials Science and Engineering, Jilin Jianzhu University, Changchun* 130118, *China*
[2] *Beijing Computational Science Research Center, Beijing* 100193, *China*

(Received 18 June 2019; revised manuscript received 8 July 2019; published online 25 July 2019)

CdTe is one of the leading materials for low cost, high efficiency thin-film solar cells with a nearly ideal band gap of 1.48 eV. However, its solar to electricity power conversion efficiency (PCE) is hindered by the relatively low open circuit voltage (V_{OC}) due to intrinsic defect related issues. Here, we propose that alloying CdTe with CdSe could possibly improve the solar cell performance by reducing the "ideal" band gap of CdTe to gain more short-circuit current from long-wavelength absorption without sacrificing much V_{OC}. Using the hybrid functional calculation, we find that the minimum band gap of the $CdTe_{1-x}Se_x$ alloy can be reduced from 1.48 eV at $x = 0$ to 1.39 eV at $x = 0.32$, and most of the change come from the lowering of the conduction band minimum. We also show that the formation of the alloy can improve the p-type doping of Cu_{Cd} impurity based on the reduced effective formation energy and nearly constant effective transition energy level, thus possibly enhance V_{OC}, thus PCE.

Keywords: alloy, bowing effect, doping, II–VI semiconductors

PACS: 61.66.Dk, 61.72.J–, 61.72.Bb, 61.72.uj **DOI:** 10.1088/1674-1056/28/8/086106

1. Introduction

CdTe is one of the leading material for low-cost, high-efficient, thin film solar cells due to its good optoelectronic property and the easy way to fabricate.[1] Although the power conversion efficiency (PCE) of the CdTe-based solar cell has so far reached to an impressive 22.1%, it is still much below the Shockley–Queisser limit (32%).[2] The current PCE in the world-record solar cell is mainly limited by the small open-circuit voltage (V_{OC}), which is about 0.85 V compared to its band gap of 1.48 V at room temperature, as well as the relatively low short-circuit current (J_{SC}), which reaches about 28 mA/cm^2 compared to $J_{SC} = 30$ mA/cm^2 under the Shockley–Queisser limit.[1,3] Currently, most efforts to improve CdTe-based solar cell efficiency have been trying to improve V_{OC} instead of the J_{SC} because of the large deficiency in V_{OC}. Some success has been achieved in increasing V_{OC} by group V doping in CdTe.[4] However, it is still not clear whether such approach can obtain stable p-type absorbers because non-equilibrium doping process has to be used to improve the p-type doping.[5] On the other hand, one may increase the PCE by increasing J_{SC}, which can be easily achieved by reducing the band gap of CdTe to harvest more long-wavelength sunlight. For example, if the band gap is reduced from 1.48 eV to 1.35 eV, the ideal J_{SC} is increased from 30 mA/cm^2 to $\sim$ 36 mA/cm^2. Because V_{OC} of the current champion CdTe solar cell is still much lower than the band gap,[6,7] mainly due to the low carrier density in p-type CdTe, reducing the band gap of CdTe slightly, especially lowering the conduction band energy, is not expected to cause much decrease of the V_{OC}.

Band gap tuning through alloying is widely used in semiconductors. Alloying CdTe at cation site could hardly achieve the reduction of the band gap, because the band gap always becomes wider when Cd is substituted by isovalent Zn,[8,9] and it is not desired to try alloying HgTe with CdTe given the toxicity of Hg. Therefore, one can only try to reduce the band gap of CdTe through alloying CdTe at anion site. The band gap of CdS and CdSe is 2.52 eV and 1.74 eV, respectively.[10] Although the band gap of CdS and CdSe are both larger than that of CdTe, alloying CdS or CdSe into CdTe can effectively reduce its band gap due to the large bowing effect.[11] Because the lattice mismatch between CdS and CdTe is large, the solubility of S into CdTe is low, which has been confirmed by previous theoretical and experimental studies.[11–13] Therefore, alloying CdTe with CdSe forming $CdTe_{1-x}Se_x$ seems to be the best choice to reduce the band gap effectively. Some of the recent experimental studies has already shown that diffusing CdSe into CdTe layer enables the increase of the J_{SC}.[2,14–16] However, so far, it is not clear how low the band gap of $CdTe_{1-x}Se_x$ could be to maximize the increase of the J_{SC}, although different experimental results regarding the $CdTe_{1-x}Se_x$ alloys have been reported.[17–21]

*Project supported by the National Key Research and Development Program of China (Grant No. 2016YFB0700700), the National Natural Science Foundation of China (Grant Nos. 51672023, 11847043, 11634003, and U1530401), and the Science Challenge Project (Grant Nos. TZ2016003 and TZ2018004) .

†Corresponding author. E-mail: suhuaiwei@csrc.ac.cn

© 2019 Chinese Physical Society and IOP Publishing Ltd

Furthermore, high p-type doping in CdTe is usually required for its solar cell performance, because as a minority carrier device, its electron mobility is much higher than the hole mobility. Although the dominant intrinsic p-type defect in CdTe is V_{Cd}, the obtained hole carrier density is too low for a good solar cell because V_{Cd} has high formation energy. Therefore, extrinsic p-type dopants, such as Cu_{Cd}, is often used in commercial CdTe-based solar cells.[22–24] However, it is also not clear how the formation of $CdTe_{1-x}Se_x$ alloy affects the doping properties in CdTe.

In this work, using the first principle hybrid-functional calculations, we find that the minimum of the band gap of the $CdSe_xTe_{1-x}$ alloy can approach 1.39 eV at about $x = 0.32$, and most of the band gap reduction is through the lowering of the conduction band minimum. Our investigation of the doping property of the alloy reveals that the formation of the impurity Cu_{Cd} exhibits dramatic bowing effect on the impurity formation energy, which can be utilized to improve the Voc, thus the PCE. The obtained band structure and the defect properties of the $CdSe_xTe_{1-x}$ alloy suggest that $CdSe_xTe_{1-x}$ alloy should be a better solar cell absorber than CdTe for the thin film solar cell application.

2. Computational methods

The first principle calculation in this work is performed by the VASP code.[25,26] PAW psuedopotentials with an energy cutoff of 350 eV were employed. PBEsol functional[27] with generalized gradient approximation (GGA) exchange correlation is used for the structure optimization of the bulk constitutes and alloys. All the atoms and the lattice vectors were fully relaxed until the force on each atom is less than 0.01 eV/Å. For the defect calculation, the lattice vectors of the optimized alloy are fixed with all the atoms inside the supercell relaxed. To calculate the band structures and the band offsets, we have employed the hybrid functional[28] consists of 32% exact Hartree–Fock exchange mixed with 68% PBE exchange with spin–orbit coupling (SOC) to determine the band gap. This specific functional is chosen so that the calculated band gap of both zinc blende CdTe and CdSe are close to experimental values. Using the proposed functional, the calculated band gaps of zinc blende CdTe and CdSe are 1.52 eV and 1.69 eV, respectively, compared to the experiment values of 1.48 eV and 1.74 eV at room temperature.[10] The calculation of the band offsets of the series of $CdSe_xTe_{1-x}$ alloys follows the method described in our previous study.[11]

The $CdSe_xTe_{1-x}$ alloy is assumed to be random and is mimicked by the special quasirandom structures (SQS)[29] in the cubic supercell of 512 or 64 atoms, when $x = 0$, 0.25, 0.5, 0.75, and 1. The cubic supercell of 512 and 64 atoms are optimized with equivalent k-point sampling of $1\times1\times1$ and $2\times2\times2$, respectively. The averaged atomic correlation functions of the first neighbor pairs, triangles and tetrahedral of the SQS are the same as the perfect random alloys in the 512-atom supercells for all the mentioned concentrations. For the 64-atom supercell, the averaged atomic correlation functions of the first neighbored tetrahedral deviates from the perfect random alloys by 0.06 for $x = 0.25$ and $x = 0.75$ but is accurate enough for this case. The way to calculate the defect formation energy and the transition energy level is the same as stated in the previous work.[30–32] After testing with different functionals and supercells, the calculated formation energies are similar, and the calculated transition energy levels are converged to within 0.03 eV. Therefore, PBEsol functional and 64-atom supercells are adopted for the calculation of the doped alloys to reduce the computational cost.

3. Results and discussion

As described above, we have calculated the respective volume and mixing enthalpy $\Delta H_{\rm mix}$ of the random $CdSe_xTe_{1-x}$ alloys with Se composition $x = 0$, 0.25, 0.5, 0.75, and 1 as shown in Figs. 1(a) and 1(b). The obtained lattice constant is 6.55 Å and 6.13 Å for pure CdTe and CdSe, respectively, in reasonably good agreement with experiment data.[10] As x increases, the volume of the $CdSe_xTe_{1-x}$ alloy decrease linearly due to the smaller size of Se, following the Vegard's rule.[33] The $\Delta H_{\rm mix}$ of the random alloy is defined as the energy difference between the $CdSe_xTe_{1-x}$ alloy and the pure CdSe and CdTe with the corresponding ratio. The calculated $\Delta H_{\rm mix}$ can be described quite well by the quadratic function $\Omega x(1-x)$, with the interaction parameter $\Omega = 76.1$ meV/f.u. Using the calculated value of Ω, the transition temperature is estimated to be 441 K, which is much lower than the experimental growth temperature,[16] therefore, it is easy to alloy CdSe into CdTe. In addition, the mixing enthalpy for $x = 0.25$ is slightly lower than for $x = 0.75$, reflecting the fact that it is easier to mix Se into CdTe than Te into CdSe.

The band gaps of the random $CdSe_xTe_{1-x}$ alloy are conventionally fitted to the equation:

$$\begin{aligned} &E_{\rm g}\,(CdSe_xTe_{1-x}) \\ &= (1-x)\,E_{\rm g}\,(CdTe) + xE_{\rm g}\,(CdSe) - bx(1-x), \end{aligned} \tag{1}$$

where b is the bowing coefficient for the band gap. The hybrid functional calculated band gaps as function of the composition x are plotted in Fig. 2(a), where the band gap bowing parameter b is found to be 0.725 eV and the band gap minimum is found at $x = 0.38$. Given the slight difference of the calculated and experimental band gaps, the composition for the band gap minimum also slightly varies. Using the calculated bowing parameter $b = 0.725$ and the experimental value of the band gaps at room temperature, the obtained band gap minimum

of the random $CdSe_xTe_{1-x}$ alloy is predicted to be 1.39 eV at $x = 0.32$, in agreement with a recent experiment result.[20]

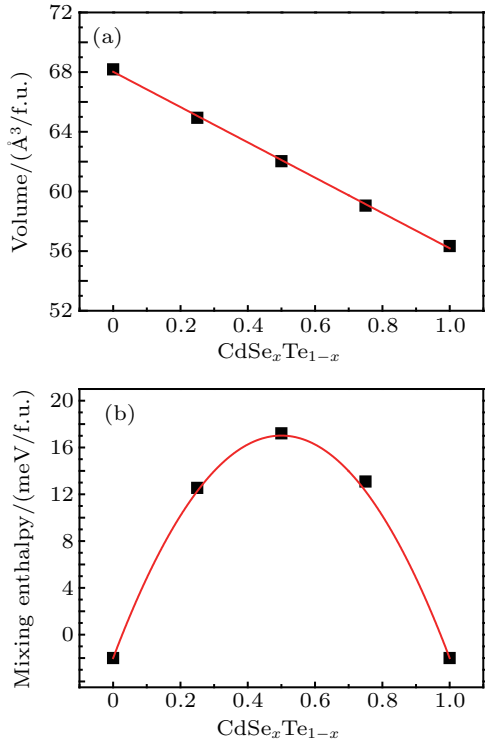


Fig. 1. The volume in units Å^3/f.u. (a) and the mixing enthalpy $\Delta H_{\rm mix}$ in units meV/f.u. (b) as the function of the composition x for $CdSe_xTe_{1-x}$ alloys. The red lines in panels (a) and (b) are fitted curves.

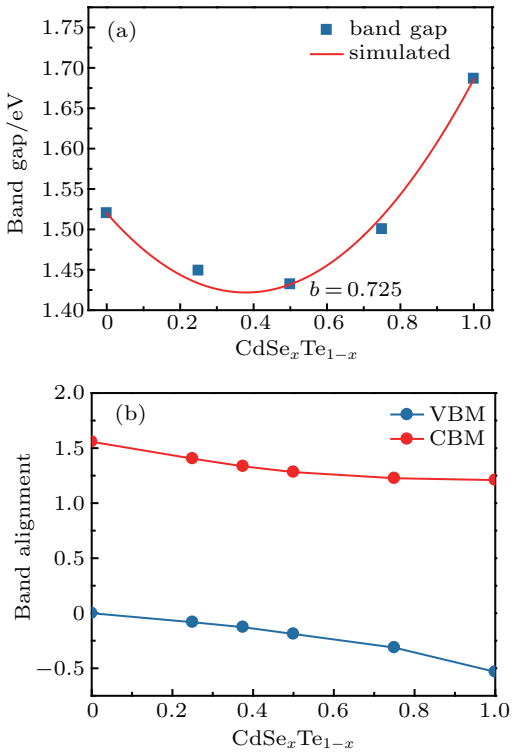


Fig. 2. (a) The calculated band gaps as a function of x for $CdSe_xTe_{1-x}$ alloys, (b) The band alignments of the $CdSe_xTe_{1-x}$ alloys as a function of x.

The bowing of the band gaps for $CdSe_xTe_{1-x}$ alloys is caused by the bowing of both the band edges. As shown in Fig. 2(b), the band offsets of the valence band minima (VBMs) and the conduction band minima (CBMs) between pure CdTe ($x = 0$) and CdSe ($x = 1$) are estimated to be 0.53 eV and 0.35 eV, respectively, consistent with the previous result.[11] Due to the strong intra valence band and intra conduction band coupling, the VBMs bow upwards and the CBMs bow downwards as x increases from 0 to 1, resulting the minimum band gap occurs at $x_{\rm min}$. At this specific concentration, the CBM bows 0.09 eV more than the VBM does. The type-II band alignment between CdTe and $CdSe_xTe_{1-x}$ suggests that a gradient $CdSe_xTe_{1-x}$ cell with Se-rich alloy in the front can help separate photogenerated electrons and holes, thus further improve the cell performance.

We first investigate the formation of the impurity Cu_{Cd} in $CdSe_{0.375}Te_{0.625}$ alloy modeled by a 64-atom SQS containing all five type $Se_{4-n}Te_n$ ($n = 0$–4) nearest neighbor motifs around each Cd atom. The formation energy of Cu_{Cd} under Cd-rich condition at each possible site are calculated and plotted in Fig. 3(a). The formation energies of Cu_{Cd} at charge state 0 and -1 depend mostly on the first neighbored configuration, although the farther neighbor configuration also has some effect, leading to the scattered formation energy within a given first neighbored motif. The averaged formation energies of the defect in different first neighbor motifs are shown in Fig. 3(b). It is obvious that the averaged formation energy increases as the number of Se atoms increase in its first neighbor. As more Se atoms surround the impurity in the first neighbor motif, the bonding orbitals of the impurity contains more Se 4p orbitals, which has lower orbital energy [Fig. 2(b)], thus, to form Cu_{Cd} state, it will cost more energy to create a hole.[34] The formation energy of Cu_{Cd}^{-1} (Fig. 3(b) top) follows the trend of its neutral state (Fig. 3(b) bottom), indicating the transition energy level $\varepsilon(0/-1)$ for Cu_{Cd} is less sensitive to its local configuration compared to the neutral formation energy. In other word, the Cu_{Cd} defect is more like a delocalized defect in $CdSe_xTe_{1-x}$ alloys.

In alloys, the defect formation energy $\Delta H_{\rm f}(\alpha, q, s, x)$ of defect α depends on charge state q, doping site s and the alloy composition x. To statistically investigate the defect property, it is more convenient to introduce an effective formation energy[35] $\Delta H_{\rm eff}(\alpha, q, x, T)$, which is x- and T-dependent weighted average of the formation energy as given in Eq. (2), where $k_{\rm B}$ is the Boltzmann constant, and N is the total number of the corresponding defect sites in alloys. To obtain the effective formation energy at charge states 0 and q, we could also define the effective transition energy level $\varepsilon_{\rm eff}(\alpha, 0/q, x, T)$ for defect α, which is the Fermi energy at which defect α at charge state 0 and q has the same effective formation energy as shown in Eq. (3).

$$\exp\left[-\Delta H_{\rm eff}(\alpha,q,x,T)/k_{\rm B}T\right] = \frac{1}{N}\sum \exp[-\Delta H_{\rm f}(\alpha,q,s,x)/k_{\rm B}T], \quad (2)$$

$$\varepsilon_{\rm eff}(\alpha,0/q,x,T) = [\Delta H_{\rm eff}(\alpha,0,x,T) - \Delta H_{\rm eff}(\alpha,q,x,T) + qE_{\rm f}]/q. \quad (3)$$

Considering the limit condition for the effective formation energy, equations (2) and (3) can be further deduced. At high temperature limit ($T \to \infty$), all the sites has equal weight, thus the effective formation energy $\Delta H_{\rm eff}(\alpha, q, x, \infty)$ is just the arithmetic average of the formation energies at all sites, so is the effective transition energy level $\varepsilon_{\rm eff}(\alpha, 0/q, x, \infty)$.

$$\Delta H_{\rm eff}(\alpha,q,x,\infty) = \frac{1}{N}\sum \Delta H_{\rm f}(\alpha,q,s,x),$$
$$\varepsilon_{\rm eff}(\alpha,0/q,x,\infty) = \frac{1}{N}\sum \varepsilon_{\rm eff}(\alpha,0/q,s,x). \quad (4)$$

On the other hand, at low temperature limit ($T \to 0$), only the site with the lowest formation energy at charge q (s_0^q) is occupied under equilibrium condition, so the effective formation energy $\Delta H_{\rm eff}(\alpha, q, x, 0)$ is just equal to $\Delta H_{\rm f}(\alpha, q, s_0^q, x)$. The effective transition energy level $\varepsilon_{\rm eff}(\alpha, 0/q, x, 0)$, therefore, is the energy difference between $\Delta H_{\rm f}(\alpha, 0, s_0^0, x)$ and $\Delta H_{\rm f}(\alpha, q, s_0^q, x)$. It is noted that the s_0^0 and s_0^q may not be at the same site.

$$\Delta H_{\rm eff}(\alpha,q,x,0) = \Delta H_{\rm f}\left(\alpha,q,s_0^q,x\right),$$
$$\varepsilon_{\rm eff}(\alpha,0/q,x,0) = \left[\Delta H_{\rm f}\left(\alpha,0,s_0^0,x\right) - \Delta H_{\rm f}\left(\alpha,q,s_0^q,x\right) + qE_{\rm f}\right]/q. \quad (5)$$

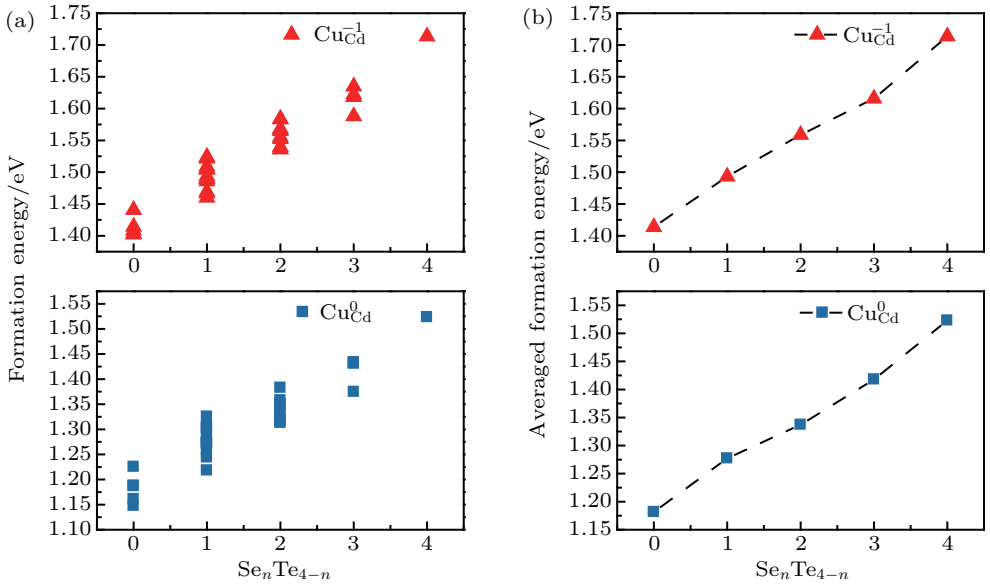


Fig. 3. (a) The formation energies of Cu_{Cd}^{-1} and Cu_{Cd}^{0} at each site in $CdSe_{0.375}Te_{0.625}$ alloy as a function of the number of the first neighbor Se atoms (n) around the impurity. (b) The arithmetic averaged formation energies of Cu_{Cd}^{-1} and Cu_{Cd}^{0} as a function of n. The black dashed line is just for guiding the eye. The Fermi level is set as 0 in both panels (a) and (b).

The calculated effective formation energies for the defect Cu_{Cd} at neutral and -1 states in $CdSe_xTe_{1-x}$ alloys ($x = 0$, 0.25, 0.375, 0.5, 0.75, and 1) at the low temperature limit, the high temperature limit and a finite temperature $T = 600$ K are shown in Figs. 4(a) and 4(b), respectively. It is interesting to see that the effective formation energy for Cu_{Cd} impurity exhibits a large bowing, *i.e.*, they are much smaller than that of the composition averaged values in the pure CdTe and the pure CdSe. This is because, in addition to the electronic effect discussed above, the strain effect also plays an important role. The formation of Cu_{Cd} causes a compressive strain due to the smaller radius of Cu than Cd, thus the formation energy of Cu_{Cd} will be reduced as the local volume surround Cu is reduced.[36] This is the case when Cu is surrounded by Te and $CuTe_4$ cluster is compressed in the $CdSe_xTe_{1-x}$ alloy, so the formation energy of Cu_{Cd} is much lower in the $CdSe_xTe_{1-x}$ alloy than in pure CdTe. The formation energy of Cu_{Cd} also decreases at the Se rich end when the $CuTe_4$ cluster is compressed most. At low temperature limit, Cu only occupy the lowest energy site ($CuTe_4$ cluster), so the bowing is the largest at the Se-rich side. At high temperature limit, the substitution occurs equally at all sites, so the effective formation energy change more smoothly as Se concentration increases. The formation of the Cu_{Cd}^{-1} generally follows the trend of Cu_{Cd}^{0} except that the bowing for Cu_{Cd}^{-1} is less dramatic than the bowing for Cu_{Cd} due to the larger size of the Cu_{Cd}^{-1} impurity.

As expected, the effective transition energy level increases as Se concentration increases in the alloy. It is interesting to see in Fig. 4(c) that at a given composition the effective transition energy level decreases as the temperature increase. This is because at the low temperature, the site with lower formation energy is preferentially occupied, where the impurity energy level for Cu_{Cd}^{0} is usually high to easily creating the hole. Therefore, the transition energy level $(0/-1)$ is relatively high. At the high temperature limit, all the defect sites have nearly equal occupation probability, so the averaged effective transition energy is reduced. However, the variation of the effective transition energy is small at a given composition (~ 0.04 eV), reflecting that Cu_{Cd} is a relatively delocalized defect in $CdSe_xTe_{1-x}$ alloys.

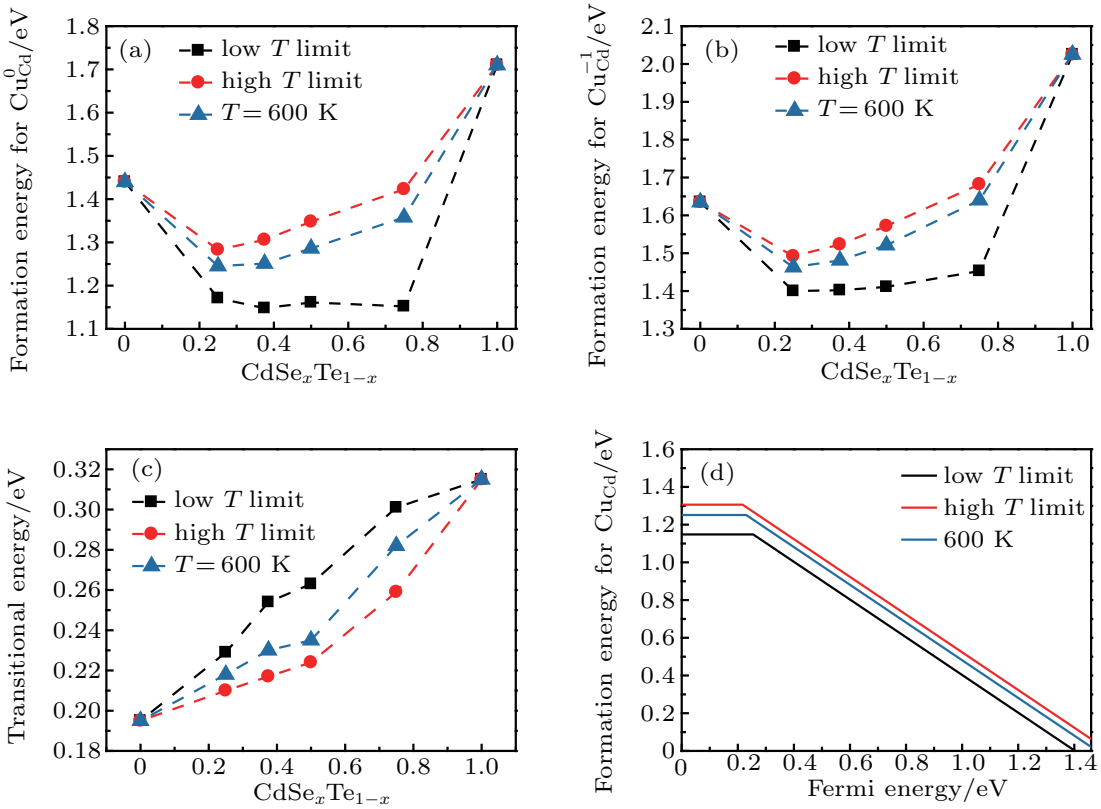


Fig. 4. The effective formation energies of Cu^0_{Cd} (a), Cu^{-1}_{Cd} (b) and the corresponding effective transition energy level (c) in $CdSe_xTe_{1-x}$ alloys ($x = 0$, 0.25, 0.375, 0.5, 0.75, and 1) at the low temperature limit, the high temperature limit, and a finite temperature $T = 600$ K. The Fermi level in panel (b) is set at 0. (d) The effective formation energy of Cu_{Cd} as a function of the Fermi energy in the $CdSe_{0.375}Te_{0.625}$ alloy at the low temperature limit, the high temperature limit, and a finite temperature $T = 600$ K.

The formation energy of the Cu^0_{Cd} defect in the $CdSe_{0.375}Te_{0.625}$ alloy range from 1.31 eV to 1.15 eV at Cd-rich limit with the transition energy level varying from 0.217 eV to 0.254 eV, depending on the synthetic temperature, as shown in Fig. 4(d). The insensitivity of the transition energy level and the lower formation energy of Cu_{Cd} in the $CdSe_{0.375}Te_{0.625}$ alloy suggests Cu doping in the alloy is more effective than that in pure CdTe.

4. Conclusion and perspectives

In summary, using first-principles calculations, we show that alloying CdTe with CdSe to form $CdSe_xTe_{1-x}$ alloys could be an effective approach to increase the PCE of the CdTe based thin film solar cells. The $CdSe_xTe_{1-x}$ alloy has two merits compared to CdTe: (i) reduced band gap (estimated to be 1.39 eV at $x = 0.32$) to improve long-wavelength light harvest, thus improving J_{SC}, (ii) lower formation energy of the shallow defect Cu_{Cd} to improve the p-type conductivity, thus the potential to improve the Voc.

Acknowledgment

We acknowledge the computational support from the Beijing Computational Science Research Center.

References

[1] Green M A, Hishikawa Y, Dunlop E D, Levi D H, Hohl-Ebinger J and Ho-Baillie A W Y 2018 *Prog. Photovolt. Res. Appl.* **26** 3
[2] Duggal A R, Shiang J J, Huber W H and Halverson A F (US Patent) US20140373908A1 [2014-12-25]
[3] Geisthardt R M, Topic M and Sites J R 2015 *IEEE J. Photovolt.* **5** 1217
[4] Burst J M, *et al.* 2016 *Nat. Energy* **1** 16015
[5] Yang J H, Yin W J, Park J S, Burst J, Metzger W K, Gessert T, Barnes T and Wei S H 2015 *J. Appl. Phys.* **118** 025102
[6] Green M A, Keith E, Yoshihiro H, Wilhelm W and Dunlop E D 2012 *Prog. Photovolt. Res. Appl.* **20** 606
[7] Green M A, Keith E, Yoshihiro H, Wilhelm W and Dunlop E D 2015 *Prog. Photovolt. Res. Appl.* **23** 805
[8] Wei S H and Zunger A 1991 *Phys. Rev. B* **43** 1662
[9] Wang Y, Xu J, Ren P, Zhuang X, Zhou H, Zhang Q, Zhu X and Pan A 2013 *Mater. Lett.* **105** 90
[10] Madelung O 1982 *Semiconductors: Basic Data*, 2nd edn. (Berlin: Springer)
[11] Wei S H, Zhang S B and Zunger A 2000 *J. Appl. Phys.* **87** 1304
[12] Yang X, *et al.* 2016 *Mater. Sci. Semicond. Process.* **48** 27
[13] McCandless B E, Hanket G M, Jensen D G and Birkmire R W 2002 *J. Vac. Sci. Technol. A* **20** 1462
[14] Paudel N R and Yan Y 2014 *Appl. Phys. Lett.* **105** 183510
[15] Paudel N R, Poplawsky J D, Moore K L and Yan Y 2015 *IEEE J. Photovolt.* **5** 1492
[16] Poplawsky J D, Guo W, Paudel N, Ng A, More K, Leonard D and Yan Y 2016 *Nat. Commun.* **7** 12537
[17] Islam R, Banerjee H D and Rao D R 1995 *Thin Solid Films* **266** 215
[18] Tit N, Obaidat I M and Alawadhi H 2009 *J. Phys.: Condens. Matter* **21** 075802
[19] Wen S, *et al.* 2017 *Nanomater. (Basel)* **7** 380
[20] Lingg M, Spescha A, Haass S G, Carron R, Buecheler S and Tiwari A N 2018 *Sci. Technol. Adv. Mater.* **19** 683

[21] MacDonald B I, Martucci A, Rubanov S, Watkins S E, Mulvaney P and Jasieniak J J 2012 *ACS Nano* **6** 5995
[22] Perrenoud J, Kranz L, Gretener C, Pianezzi F, Nishiwaki S, Buecheler S and Tiwari A N 2013 *J. Appl. Phys.* **114** 174505
[23] Kranz L, *et al.* 2013 *Nat. Commun.* **4** 2306
[24] Bätzner D L, Romeo A, Zogg H, Wendt R and Tiwari A N 2001 *Thin Solid Films* **387** 151
[25] Kresse G and Furthmüller J 1996 *Comput. Mater. Sci.* **6** 15
[26] Kresse G and Furthmüller J 1996 *Phys. Rev. B* **54** 11169
[27] Perdew J P, Ruzsinszky A, Csonka G I, Vydrov O A, Scuseria G E, Constantin L A, Zhou X and Burke K 2008 *Phys. Rev. Lett.* **100** 136406
[28] Krukau A V, Vydrov O A, Izmaylov A F and Scuseria G E 2006 *J. Chem. Phys.* **125** 224106
[29] Wei S H, Ferreira L G, Bernard J E and Zunger A 1990 *Phys. Rev. B* **42** 9622
[30] Ma J, Wei S H, Gessert T A and Chin K K 2011 *Phys. Rev. B* **83** 245207
[31] Yang J H, Chen S, Xiang H, Gong X G and Wei S H 2011 *Phys. Rev. B* **83** 235208
[32] Yang J H, Yin W J, Park J S, Ma J and Wei S H 2016 *Semicond. Sci. Technol.* **31** 083002
[33] Vegard L 1921 *Z. Phys.* **5** 17
[34] Deng H X, Luo J W, Wei S H 2018 *Chin. Phys. B* **27** 117104
[35] Ma J and Wei S H 2013 *Phys. Rev. B* **87** 241201
[36] Zhu J, Liu F, Stringfellow G B and Wei S H 2010 *Phys. Rev. Lett.* **105** 195503